

Exploring the Capabilities and Limits of 3D Monocular Object Detection - A Study on Simulation and Real World Data

Felix Nobis¹, Fabian Brunhuber², Simon Janssen², Johannes Betz¹ and Markus Lienkamp¹

Abstract—3D object detection based on monocular camera data is a key enabler for autonomous driving. The task however, is ill-posed due to lack of depth information in 2D images. Recent deep learning methods show promising results to recover depth information from single images by learning priors about the environment. Several competing strategies tackle this problem. In addition to the network design, the major difference of these competing approaches lies in using a supervised or self-supervised optimization loss function, which require different data and ground truth information. In this paper, we evaluate the performance of a 3D object detection pipeline which is parameterizable with different depth estimation configurations. We implement a simple distance calculation approach based on camera intrinsics and 2D bounding box size, a self-supervised, and a supervised learning approach for depth estimation.

Ground truth depth information cannot be recorded reliable in real world scenarios. This shifts our training focus to simulation data. In simulation, labeling and ground truth generation can be automatized. We evaluate the detection pipeline on simulator data and a real world sequence from an autonomous vehicle on a race track. The benefit of simulation training to real world application is investigated. Advantages and drawbacks of the different depth estimation strategies are discussed.

I. INTRODUCTION

Today’s most accurate 3D object detection methods make use of LIDAR sensor data [1], [2], [3] and surpass monocular object detection methods by a great margin on the KITTI data set [4]. The leading lidar algorithm [1] achieves a 3D Average Precision (AP) of 81.43 % in the car category, whereas the leading monocular estimator [5] achieves a 3D AP of 11.72 %. Regarding 2D object detection metrics, lidar and camera detection algorithms achieve comparable performance [4]. The disadvantage of the camera sensors is the lack of 3D depth information in the 2D image representation. Nonetheless, object detection on a single camera sensor comes with numerous advantages, leading to broad research interest in the field in the recent years: In contrast to lidar sensors, the hardware availability of cameras for autonomous driving is greater due to lower sensor costs. The roads are designed for human vision which has a great comparability to camera data. The feature density in the camera data is greater than the one of the sparse lidar detections, which comes with a greater potential for the detection possibility.

¹Felix Nobis (corresponding author), Johannes Betz and Markus Lienkamp are with the Chair of Automotive Technology, Technical University of Munich nobis@ftm.mw.tum.de

²Fabian Brunhuber, Simon Janssen are master students at the Technical University of Munich

Furthermore, camera and lidar detection algorithms can be developed in a redundant manner, increasing the fault tolerance of the complete autonomous software stack. In the development process, a separated development for the different sensor modalities can lessen the overall complexity as the sensor specific development teams can work in their field of expertise independently. Early fusion approaches [6], [7], [8], while showing a great potential due to higher information density, come with the organizational drawback of requiring the knowledge of different sensor modalities at a low abstraction level in the whole team.

In this paper, we apply monocular 2D object detection and monocular depth estimation in a parallel pipeline to perform 3D object detection. Two stage 3D detection pipelines have been applied for example in [9]. In comparison, we use a more simple approach, which estimates the depth of 2D bounding box detections and calculates the 3D position without estimating the full 3D pose. We compare three different depth estimation pipelines and evaluate their 3D position estimation performance on simulation and real world image data. An overview of the alternative detection pipeline configurations is given in Figure 1.

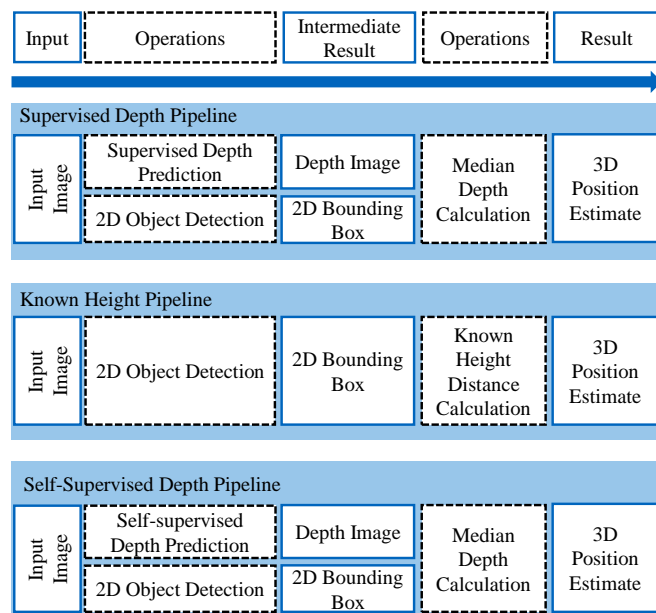


Fig. 1. 3D object detection pipeline with three alternative configurations.

The detection performance is evaluated for the continuous trajectory of a race car on the track in simulation and in a real world scenario. The real world scenario was recorded

in the context of the Roborace autonomous racing challenge [10], [11].

Collecting appropriate data and labelling them correctly for camera learning algorithms can be tedious and error-prone. It would be beneficial if no extensive data collection and labelling strategy is necessary by using simulation data. Our work discusses the current drawbacks of bridging the domain gap between simulation and real world data. It hints to the potential to use simulation to adapt deep learning approaches for real world data sets.

Section II discusses depth estimation, monocular object detection and simulation environments for autonomous driving. Section III presents the object detection pipeline developed in this work. Additionally, it gives insight to the data generation and data handling process with the simulator. The evaluation and discussion of the approach is performed in Section IV. Finally, our conclusions from the work are presented in Section V.

II. RELATED WORK

In this section, we present the state of the art of: Monocular depth estimation, 2D monocular object detection and simulation environments for autonomous driving research.

A. Monocular Depth Estimation

Depth inference from monocular images is ill-posed. In recent years, different approaches emerged to deal with the lack of 3D information in images and to reconstruct the 3D scene [12], [13], [14], [15], [16], [17], [18]. The methods can be categorized as either supervised learning methods, which require ground-truth depth information, or self-supervised learning methods, which only require RGB images for training.

[14] reconstructs the monocular depth by learning the disparity for a virtual stereo setup from stereo image ground truth data. At inference time, only a monocular camera is necessary to reconstruct the 3D information.

[15] uses consecutive frames from a monocular camera to reconstruct adjacent frames through a neural network. The loss is constructed as an image reconstruction problem without an explicit depth term, thereby it does not require depth ground truth. To be able to reconstruct the frames, the network learns the transformation of the camera viewpoint explicitly and thereby also provides a source of odometry information. [16] augments their network to explicitly handle moving objects in the depth prediction. In the previous approaches, especially the depth estimation of objects moving at a similar speed as the camera resulted in those objects to be wrongly mapped to infinity. [19] extends this method in a way that it learns the intrinsic parameters of the source camera in addition to the depth estimate.

The currently best performing network on the KITTI leaderboard is DORN [17] which uses an ordinal loss to calculate the depth for different discrete intervals. The rationale behind this is to augment the influence of near depth values in the loss calculation, which are outweighed in

the previous formulations by far depth values and increased depth estimation errors.

DenseDepth [18] present a loss function which takes the gradient of the depth into account for the loss calculation. This tackles the problem of edge-bleeding around the contours of objects. The shown performance metrics are slightly worse than the ones of DORN for the KITTI data set, while they surpass them for the NYU Depth v2 data set [20]. The authors explain the worse performance on KITTI with the sparse ground truth information depth information in this data set.

B. Monocular 2D Object Detection

Object detection on the 2D image space with deep learning method has seen a strong interest after early promising results of Overfeat [21] and R-CNN [22]. An extensive review of 2D object detection methods is found in [23] and [24].

C. Simulation Environments

A variety of simulation environments exists for the development of autonomous driving features [25], [26], [27], [28], [29]. [30] gives a further overview of perception systems and simulation environments. The use of simulation in the development of perception systems facilitates the data generation process. In simulation, a greater variety of scenes can be modeled. Edge cases [31] can be introduced explicitly into the data set. Additionally, the explicit modelling in the simulation enables the automatic generation of ground truth information. This is a great advantage to the time consuming or costly manual labelling for real world data sets [32], [33]. While the usage of simulation and the benefits to real world perception are on a rise, current simulations still do not represent the real world environment in enough detail to make real world data collection and labeling obsolete.

III. OBJECT DETECTION DEVELOPMENT

Depth estimation is the greatest challenge in 3D object detection with current methods. We implement three different strategies for the depth estimation of objects and analyze their advantages and drawbacks:

- Distance calculation using the 2D bounding box height, and the known height of the real world race car as a geometric constraint. We call this method known height assumption.
- Depth estimation for the whole image using the supervised DenseDepth network. The distance to each object is calculated as the median depth value in the bounding box crop. Explicit knowledge about the objects, like height information, is not required in this approach.
- Depth estimation for the whole image using the self-supervised struct2depth network. The distance to each object is calculated as the median depth value in the bounding box crop. Explicit knowledge about the objects, like height information, is not required in this approach.

To generate the 2D bounding box detection, we train and employ the one-stage network SSD [34] from the Tensorflow

Object Detection API [24]. The performance of 2D object detection has been proven extensively in literature and is not the focus in this paper. For the evaluation results, we therefore mostly resort to ground truth 2D boxes to study the effect of the depth estimation isolated.

We perform 3D object detection by inferring the 3D position of the detected object by using different depth estimation strategies. In addition to the simple depth estimation we present in this paper, we employ 3D lidar detection networks [35] on the same data in the underlying project, so that we are interested in keeping the similarities between the estimated camera depth data and lidar depth data high. For this, we are especially concerned about the edge bleeding problem from monocular depth estimation. Therefore, we adapt the DenseDepth network [18] for our depth estimation pipeline. [36] states that using synthetic data for training of depth estimation networks is an open challenge. To study the effect of synthetic training data more broadly, we implement a second depth estimation network in the pipeline. We integrate the struct2depth network [16], as it is specialized to deal with object motion in the scene which occurs in the racing scenes of our use case. Furthermore, it is trained in a self-supervised manner, whereas DenseDepth requires depth ground truth information leading to a comparison of two inherently different estimation approaches. After using the depth networks, we calculate the distance to all objects detected in 2D. This is done by extracting the median depth of the 2D bounding box crop on the depth image. In the following, we describe the workings and main consideration to work with the different depth estimation approaches

A. Known Height Assumption Pipeline

The explicit distance calculation is possible since we are interested in calculating the distance to objects for which we know the real world height in meters h_{car} . Additionally we calculate the vertical focal length in pixel units F_v . The height of a 2D bounding box detection in pixel units is H_{bb} . The distance to the object in the bounding box can then be calculated using the following formula:

$$d = h_{car} * F_v / H_{bb}. \quad (1)$$

B. Depth Network Pipelines

The depth networks are trained following the training schemes from their original implementations and building on top of the publicly available network configurations trained on the KITTI data set.

1) *Self-supervised Pipeline:* The struct2depth network is trained on consecutive frames from racing scenes recorded in the simulator on two different race tracks. The camera vehicle follows the object vehicle in varying distances of up to 100 m. In total there are around 4500 frames in the simulator training data set. The data generation is somewhat limited even in simulation due to the constraint that consecutive frames are needed for the training. On the other hand the network can be trained on simulator and real world data since no ground truth depth is necessary. Therefore in

addition to the simulation data, the training data set contains around 4000 real world images.

2) *Supervised Pipeline:* The DenseDepth network is trained on simulator data on consecutive frames and additional arbitrary poses of the object vehicle. In the arbitrary scenes, the object is placed in a distance between 4 m to 100 m in front of the vehicle with arbitrary rotations between -90° to 90° relative to the ego vehicle. The poses are recorded for numerous locations around the race track to generate a great variety in the data set.

C. Computational Considerations

The simple distance calculation is computationally negligible. Whereas the depth estimation networks need additional GPU resources. For practical considerations, they can be run in parallel to the 2D object detection networks, so that the overall delay for a real time inference is the maximum of the 2D detection network and the depth estimation network inference time and not the addition of the two.

D. Simulation Design

A suitable data set must contain realistic environment conditions and sufficiently large variety in order to generalize well in the simulation and real world domain. The evaluation on the real world data is performed on a stretch of a race track which consists of a left-right curve combination and a straight. The simulation models the same race track and an additional race track from the Roborace competition from GPS locations of the real race track bounds. Additionally, videos of the race track are analyzed to create a more realistic environment replication by including trees, hills and buildings which are present along the race track. Different lighting conditions are simulated. This includes lens flare and different positioning of the sun and sky modelling. The paintwork of the race car is varied in three different setups to make the network invariant to the specific paint of the vehicle. As simulation backbone, we use the Unity environment, because of the ease-of-use of its functionalities and the appealing graphics performance.

E. Data sets

Both networks are trained on a data set generated in our Unity race simulation. The simulation environment is programmed to output the ground truth 3D poses of the ego and the object vehicles for every frame. The simulation saves images captured by a virtual camera which is configured to match the intrinsic and extrinsic parameters of the real world data set. Furthermore, it delivers the pixel-level ground truth depth and segmentation mask for the object vehicles.

The ground truth depth is saved in a 16bit PNG format. The resolution of a standard 8bit format is not fine-grained enough to store the depth information for the range of interest up to 100 m. The PNG format uses a lossless compression to prevent depth artifacts which occur in JPG images.

In the real world recording the original camera resolution is scaled down by a factor of two to enable real-time recording of the image data on the vehicle hardware. As

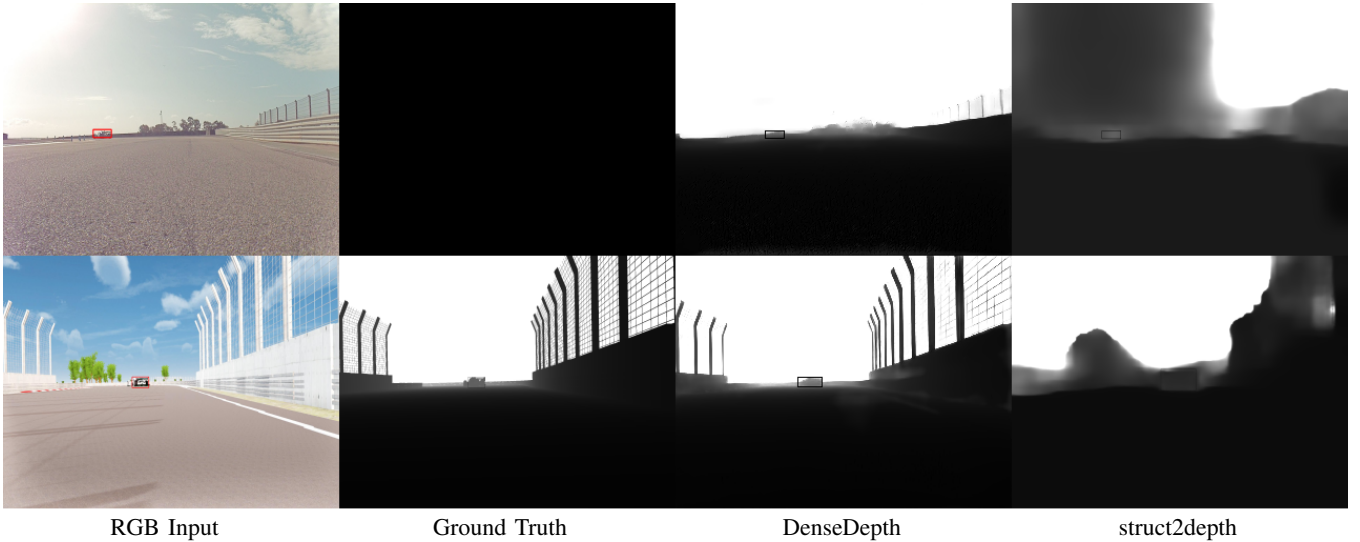


Fig. 2. Example scenes and corresponding depth images. The first row shows real world data. The second row shows simulation data.

a difference, in the simulation the full resolution of the modeled camera is used for recording and known height inference. The depth networks operate with the same down-scaled resolution for simulation and real world data.

The simulation data set contain images from two different race tracks. In the simulation training sets, the camera vehicle follows an object vehicle at arbitrary distances of up to 100 m. Furthermore, the self-supervised depth network is trained with real world race track data.

IV. EXPERIMENTS AND RESULTS

This section evaluates the results of the three different depth estimation techniques in detail on three different test sets.

A. Evaluation Metrics

The networks are evaluated regarding the 3D recall and Average Translational Error (ATE) metrics. These 3D metrics are inspired by the 3D mAP proposed by the authors of [37]. The 3D recall is the main result of the evaluation. The use of an additional precision or AP metric is not relevant here, since 2D false positives do not occur on the whole data set. All 3D false positive (FP) detections arise from errors in the distance estimation of true positives (TP) which are therefore already registered in the 3D recall metric. The ATE gives an additional insight into the absolute translational error in the ground plane for both the TP and the FP detections.

B. Evaluation

An exemplary frame from the real world test set is shown in the first row in Figure 2. Row two shows the same scene modeled in the simulation.

The test of the network is performed in three different environments:

- Test set 1 : Vehicle following sequence at distances of around 20 m in the simulation. 355 frames.
- Test set 2 : Vehicle following sequence at distances of around 70 m in the simulation. 209 frames.

- Test set 3 : Vehicle following sequence at distances of around 50 m in the real world scenario. 738 frames.

TABLE I

3D POSITION DETECTION WITH DIFFERENT PIPELINE CONFIGURATIONS. IF NOT STATED OTHERWISE, THE 2D BOUNDING BOX IS TAKEN FROM THE GROUND TRUTH BOXES. GT: GROUND TRUTH DEPTH. DD: DENSEDEPTH. S2D: STRUCT2DEPTH. KH: KNOWN HEIGHT ASSUMPTION. SSD: 2D BUNDING BOX DETECTION WITH SINGLE SHOT DETECTOR.

Test set	Depth Configuration	3D Recall in %	ATE in m
1 - Sim 20m	GT	95.99	0.2
	KH	72.32	0.8
	S2D	46.34	2.2
	DD	32.25	4.4
2 - Sim 70m	GT	90.55	0.8
	KH	55.98	1.5
	S2D	14.95	9.3
	DD	7.54	11.4
3 - Real World	KH	17.68	4.9
	S2D	2.57	23.7
	DD	2.37	15.6
	SSD KH	27.71	3.6

For each scene, we evaluate the object detection pipeline with different configurations for the distance estimation. The results are shown in Table I.

For the simulator data, we first calculate the 3D position estimation by using the ground truth 2D bounding boxes and calculating the median distance for this bounding box crop from the ground truth depth image. This is the theoretical maximum 3D recall that we can achieve with the presented 2D + depth approaches if we would be able to generate perfect depth from the image data. We do not achieve a perfect 3D recall since we compare the center of the opponent bounding box to the ground truth. Since all methods measure the distance to the back of the objects, we have to add an offset to represent the center point of the object vehicle. This

offset is known if we know the vehicle size and assume a straight heading of the vehicle in front of us. In curves however, this assumption introduces an error due to the unknown heading of the object vehicle. We do not introduce a tracking of the position and heading to mitigate this error, since we want to evaluate the raw detection performance without the augmentation of the results through tracking. The error by the center offset in a curve is shown in Figure 3.

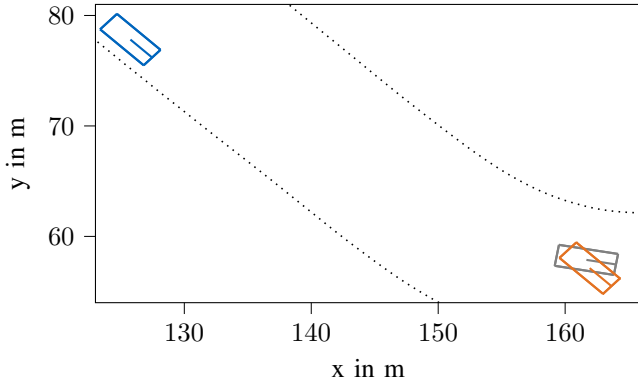


Fig. 3. The ego vehicle position is shown in blue. The detection object position in orange is calculated with ground truth 2D bounding box and ground truth depth information. Ground truth object position in gray. Due to the unknown heading of the detected vehicle, the center point detection has a slight error in the curve.

Table I shows a general decline in accuracy for an increase of the distance to the object and to the detection on real world data.

1) *Known Height Assumption Discussion:* The known height distance calculation achieves the best results over all data sets. Even though the use case of this form of distance calculation is limited and the deep learning approaches provide a lot of more information for the whole scene, it fits best for the shown use case and the available data. As a drawback of the method due to the discrete pixel size, the detection resolution declines with an increased distance of the object vehicle and with lower camera resolutions. With a camera of focal length 900 px we can detect an object of 1 m height at a distance of 50 m. The next farther detectable distance bin for the same object is at almost 53 m. As seen in Equation 1, the distance estimation scales inversely proportional to the measured pixel height. At a distance of 25 m, the next farther distance bin lies at around 25.7 m. Increasing image resolutions and thereby increasing the focal length in pixel units, increases the distance resolution. At the same time, this leads to a greater amount of raw data to process and more expensive cameras.

The resolution in our real world data set is half of the full HD solutions used in the simulator. The errors for this method are thereby increased for the real world data set. The discrete distance bins for the known height distance calculation can be observed in Figure 6. A single pixel error in height estimation, can already lead to a FP 3D detection. Additionally, the 2D bounding boxes are annotated manually and therefore the ground truth bounding box height in pixels

is not always accurate as it is in the simulation. It is interesting to note, that the 3D recall metric for the 2D bounding box generated by the SSD detection network surpasses the one of the ground truth bounding box. Concerning the height measurement, the 2D detector seems to achieve a better performance than our manual labelling. A third source of error for this method is introduced due to relative non-zero pitch angles of the detected vehicles. The 2D bounding box will naturally have a greater height if it has to encompass an inclined vehicle. Even if the 2D detection works flawless, the distance will thereby be underestimated, e.g. for a vehicle driving up a hill.

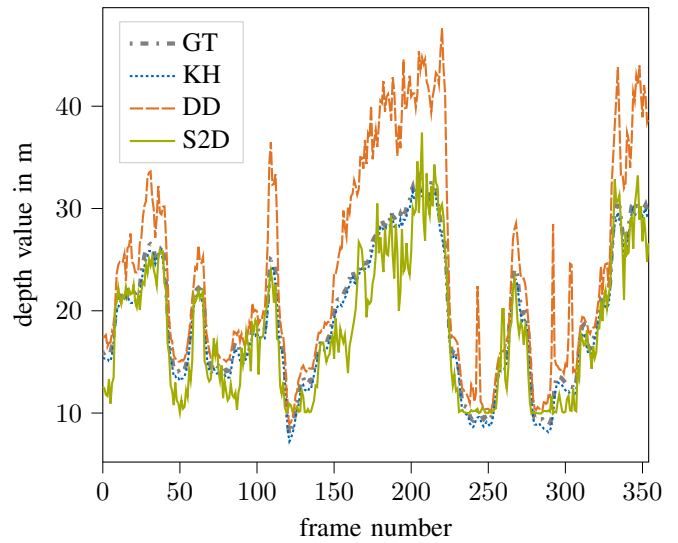


Fig. 4. Depth estimation results for simulation test set 1.

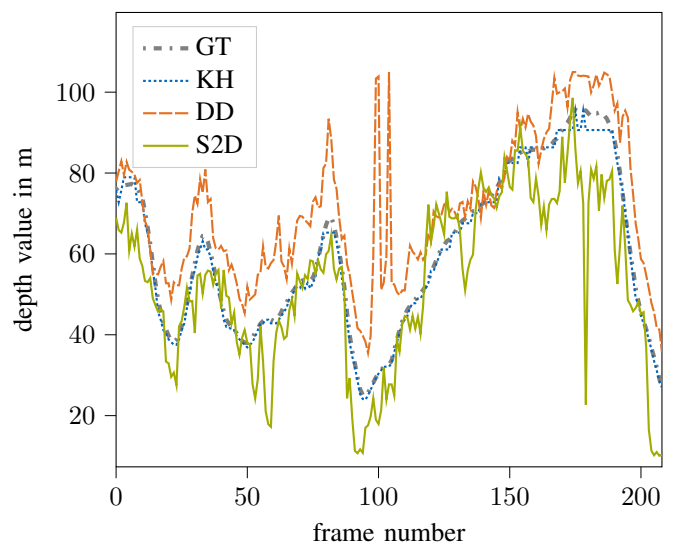


Fig. 5. Depth estimation results for simulation test set 2.

2) *Supervised Depth Discussion:* The DenseDepth estimation leads to the worst recall results. However, an optical

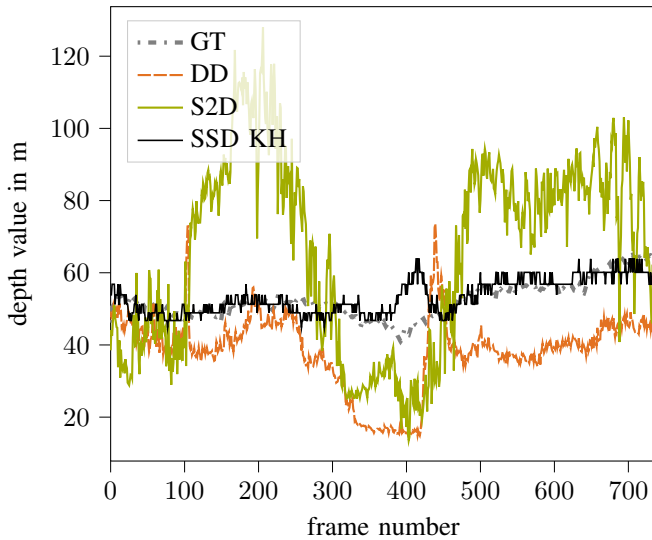


Fig. 6. Depth estimation results for real world test set 3.

assessment of the depth estimation images show a reasonable scene representation. The general distance estimation feasibility can be seen in Figures 4 and 5 for the simulator test sets. Even though the estimation is not accurate enough to achieve an accurate 3D recall metric, the general distance estimation trend follows the ground truth value for the detected object.

The distance outliers around frame 100 in Figure 5 result from images where the object vehicle is barely visible at the edge of the frame, making the depth estimation as well as the median calculation prone to greater errors.

The supervised depth pipeline overestimates the depth for most frames.

The distance error peaks in the sequence shown in Figure 4 at short distance the error peaks, are found due to artifacts in the estimated depth map which are most notably present between frames 150 to 230. The reason for these artifacts is unknown.

The appliance to the real world test data does not lead to comparable results. This is shown in Figure 6. The distance estimate is varying greatly from the ground truth. An optical inspection leaves a general consistent impression of the environment. However, the race car is less recognizable than it is for the simulation images. During the frames around 230 to 400, the vehicle is driving towards the sun. This coincides with the drop in depth detection performance. Even though similar lighting effects are modelled in the simulation, it seems the network can not generalize well to these conditions.

Additionally the object vehicle is always partly over the horizon line in the camera frame of the simulation. Due to the hilly terrain this is rarely the case in the real world sequence. An accurate terrain modelling in the simulation training data could potentially lead to better results here. The optical impression from the DenseDepth output shown in Figure

2 motivates the conclusion, that the network is generally able to learn the depth of its environment from simulation even when it is applied to real world data. However, a high variety needs to be covered in the training data set. In line with comparable depth networks, this network learns a strong prior about its environment. This comes with the drawback of weak generalizability of the results to additional data sets or unknown scenarios.

3) *Self-supervised Depth Discussion:* The struct2depth inference results in the second best recall metrics. The optical assessment of the depth images, show that the vehicle is distinguishable from the environment, however the edges are not visible clearly. Additionally, the optical impression of the environment estimation shown in Figure 2 is worse than the one of the DenseDepth. The visual appealing results from the paper could not be reproduced. The visualizations shown in the original paper seem to performs well for the close range of roughly 20 m from the vehicle, farther distances seem to be learned worse by this approach.

The detection performance in the real world data set is not promising as shown in Figure 6. Even though it is trained on images from simulation and on real world data, it can not generalize to the real world data set on testing. While the metric results are comparable, the optical impression of the scene is not as well represented as it is in the supervised approach. Similar to DenseDepth, the generalization of the network seems to be weak between the different data sets: KITTI, Unity simulation and the real world race track scenario.

V. CONCLUSIONS

This paper investigates the capabilities of monocular camera systems for 3D object detection. Firstly, a simulation environment with the Unity 3D engine is built to simulate autonomous driving scenarios on race track environments. This simulator generates image and ground truth data to train neural networks for depth estimation. An algorithmic distance calculation, a self-supervised deep learning method and supervised deep learning method are implemented to showcase limits and possibilities of 3D monocular object detection.

The depth network results can be generalized over data sets to a limited extent, e.g. general optical impression. If the camera intrinsics or resolution of the input images are changed, the level of generalizability is further reduced. The learning works only within specific conditions. Extrapolating the results to a greater amount of training data, we conclude that 3D object detection could be performed reasonable well with current methods for close range scenarios of around 20m distances. The detection performance deteriorates for greater distances. In theory this can be compensated by higher image resolutions at the cost of a higher overall data rate. Alternatively cameras with a small and wide field-of-views can be combined to enable accurate detections for additional desired ranges. Leading to higher system complexity and package requirements.

For future work, the level of detail of the simulation needs to be augmented. Especially modelling the height of the race track terrain is expected to make the depth networks perform better in real world scenarios, since the system has not seen vertical movement of the camera in the training. Even though the known height calculation showed the best performance for the application, it is not easily applicable to more general scenarios with a number of different unknown objects. In the current study, the self-supervised network showed the better overall performance in terms of metrics. The supervised approach produced a visually more consistent depth map even though the self-supervised approach was additionally trained on a real world data. The detection results after training with additional simulator details and a more diverse data set need to be investigated for both configurations.

[38] augments the KITTI data set scenes with additional object instances to generate more diverse training data. The augmentation of real world data with simulation objects is another promising approach to bridge the domain gap.

Even though there is a lot of research conducted in this direction, 3D monocular object detection is not on par with the performance of stereo camera or lidar methods even in favorable conditions for the monocular camera. The networks learn a strong prior about the environment and can create realistic 3D models for a specific environment. However, after an extensive literature research there seems to be no current model that is able to generalize well in a variety of conditions. [39] states that the accuracy of depth estimation is heavily data set depend. A real world series application of a monocular depth estimation approach therefore would need to incorporate vast amounts of training data, covering all possible future scenarios yet in the training. While this could be possible with fleet data recordings, it would still be a tedious task. With current methods, the fusion of camera information with distance measuring sensors such as lidar and radar still seems to be the most effective method to perform object detection in 3D.

CONTRIBUTIONS AND ACKNOWLEDGEMENT

Felix Nobis initiated the idea of this paper and contributed essentially to its conception and content. Fabian Brunhuber contributed to the development of the simulation environment and the training of the self-supervised depth network. Simon Janssen contributed to the implementation of the inference pipeline and the training of the supervised depth network. Johannes Betz revised the paper critically. Markus Lienkamp made an essential contribution to the conception of the research project. He revised the paper critically for important intellectual content. He gave final approval of the version to be published and agrees to all aspects of the work. As a guarantor, he accepts the responsibility for the overall integrity of the paper. We express gratitude to Continental Engineering Service for funding for the underlying research project.

REFERENCES

- [1] S. Shi, C. Guo, L. Jiang, Z. Wang, J. Shi, X. Wang, and H. Li, "Pv-rcnn: Point-voxel feature set abstraction for 3d object detection," 2019. [Online]. Available: <https://arxiv.org/pdf/1912.13192>
- [2] Z. Yang, Y. Sun, S. Liu, X. Shen, and J. Jia, "Std: Sparse-to-dense 3d object detector for point cloud," 2019. [Online]. Available: <https://arxiv.org/pdf/1907.10471>
- [3] S. Shi, Z. Wang, J. Shi, X. Wang, and H. Li, "From points to parts: 3d object detection from point cloud with part-aware and part-aggregation network," 2019. [Online]. Available: <https://arxiv.org/pdf/1907.03670>
- [4] A. Geiger, P. Lenz, and R. Urtasun, "Are we ready for autonomous driving? the kitti vision benchmark suite," in *Conference on Computer Vision and Pattern Recognition (CVPR)*, 2012. [Online]. Available: <http://www.cvlibs.net/datasets/kitti/>
- [5] M. Ding, Y. Huo, H. Yi, Z. Wang, J. Shi, Z. Lu, and P. Luo, "Learning depth-guided convolutions for monocular 3d object detection," 2019. [Online]. Available: <https://arxiv.org/pdf/1912.04799>
- [6] J. Ku, M. Mozifian, J. Lee, A. Harakeh, and S. Waslander, "Joint 3d proposal generation and object detection from view aggregation," *IROS*, 2018.
- [7] X. Chen, H. Ma, J. Wan, B. Li, and T. Xia, "Multi-view 3d object detection network for autonomous driving," 2016. [Online]. Available: <http://arxiv.org/abs/1611.07759v3>
- [8] F. Nobis, M. Geisslinger, M. Weber, J. Betz, and M. Lienkamp, "A deep learning-based radar and camera sensor fusion architecture for object detection," in *2019 Sensor Data Fusion: Trends, Solutions, Applications (SDF)*. IEEE, 2019, pp. 1–7.
- [9] Y. Wang, W.-L. Chao, D. Garg, B. Hariharan, M. Campbell, and K. Q. Weinberger, "Pseudo-lidar from visual depth estimation: Bridging the gap in 3d object detection for autonomous driving," 2018. [Online]. Available: <https://arxiv.org/pdf/1812.07179>
- [10] J. Betz, A. Wischniewski, A. Heilmeyer, F. Nobis, T. Stahl, L. Hermansdorfer, and M. Lienkamp, "A software architecture for an autonomous racecar," in *2019 IEEE 89th Vehicular Technology Conference (VTC2019-Spring)*. IEEE, 2019, pp. 1–6.
- [11] Roborace, "Roborace," 2018. [Online]. Available: <https://roborace.com/>
- [12] D. Eigen, C. Puhrsch, and R. Fergus, "Depth map prediction from a single image using a multi-scale deep network," 2014. [Online]. Available: <https://arxiv.org/pdf/1406.2283>
- [13] R. Ranftl, V. Vineet, Q. Chen, and V. Koltun, "Dense monocular depth estimation in complex dynamic scenes," in *29th IEEE Conference on Computer Vision and Pattern Recognition*. Piscataway, NJ: IEEE, 2016, pp. 4058–4066.
- [14] C. Godard, O. M. Aodha, and G. J. Brostow, "Unsupervised monocular depth estimation with left-right consistency," in *CVPR*, 2017.
- [15] R. Mahjourian, M. Wicke, and A. Angelova, "Unsupervised learning of depth and ego-motion from monocular video using 3d geometric constraints," 2018. [Online]. Available: <http://arxiv.org/pdf/1802.05522v2>
- [16] V. Casser, S. Pirk, R. Mahjourian, and A. Angelova, "Depth prediction without the sensors: Leveraging structure for unsupervised learning from monocular videos," *Thirty-Third AAAI Conference on Artificial Intelligence*, 2019.
- [17] H. Fu, M. Gong, C. Wang, K. Batmanghelich, and D. Tao, "Deep ordinal regression network for monocular depth estimation," *CoRR*, vol. abs/1806.02446, 2018.
- [18] I. Alhashim and P. Wonka, "High quality monocular depth estimation via transfer learning," 2018. [Online]. Available: <https://arxiv.org/pdf/1812.11941>
- [19] A. Gordon, H. Li, R. Jonschkowski, and A. Angelova, "Depth from videos in the wild: Unsupervised monocular depth learning from unknown cameras," 2019. [Online]. Available: <https://arxiv.org/pdf/1904.04998>
- [20] N. Silberman, D. Hoiem, P. Kohli, and R. Fergus, "Indoor segmentation and support inference from rgb-d images," in *ECCV*, 2012.
- [21] P. Sermanet, D. Eigen, X. Zhang, M. Mathieu, R. Fergus, and Y. LeCun, "Overfeat: Integrated recognition, localization and detection using convolutional networks," 2013. [Online]. Available: <https://arxiv.org/pdf/1312.6229>
- [22] R. Girshick, J. Donahue, T. Darrell, and J. Malik, "Rich feature hierarchies for accurate object detection and semantic segmentation," 2013. [Online]. Available: <https://arxiv.org/pdf/1311.2524>

- [23] Z.-Q. Zhao, P. Zheng, S.-t. Xu, and X. Wu, "Object detection with deep learning: A review," 2018. [Online]. Available: <https://arxiv.org/pdf/1807.05511>
- [24] J. Huang, V. Rathod, C. Sun, M. Zhu, A. Korattikara, A. Fathi, I. Fischer, Z. Wojna, Y. Song, S. Guadarrama, and K. Murphy, "Speed/accuracy trade-offs for modern convolutional object detectors," 2016. [Online]. Available: <http://arxiv.org/pdf/1611.10012v3>
- [25] A. Dosovitskiy, G. Ros, F. Codevilla, A. Lopez, and V. Koltun, "Carla: An open urban driving simulator," 2017. [Online]. Available: <https://arxiv.org/pdf/1711.03938>
- [26] MATLAB and Epic Games, "Vehicle dynamics blockset interface for unreal engine 4 projects," 2018. [Online]. Available: <https://www.mathworks.com/matlabcentral/fileexchange/65966-vehicle-dynamics-blockset-interface-for-unreal-engine-4-projects>
- [27] Unity Technologies, "Unity," 2019. [Online]. Available: <https://unity.com/de/solutions/automotive-transportation/autonomous-vehicle-training>
- [28] S. Shah, D. Dey, C. Lovett, and A. Kapoor, "Airsim: High-fidelity visual and physical simulation for autonomous vehicles," 2017. [Online]. Available: <https://arxiv.org/pdf/1705.05065>
- [29] IPG Automotive, "Carmaker," 2019. [Online]. Available: <https://ipg-automotive.com/de/produkte-services/simulation-software/carmaker/>
- [30] F. Rosique, P. J. Navarro, C. Fernández, and A. Padilla, "A systematic review of perception system and simulators for autonomous vehicles research," *Sensors (Basel, Switzerland)*, vol. 19, no. 3, 2019.
- [31] L. Fridman, L. Ding, B. Jenik, and B. Reimer, "Arguing machines: Human supervision of black box ai systems that make life-critical decisions," 2017. [Online]. Available: <https://arxiv.org/pdf/1710.04459>
- [32] Intel, "Computer vision annotation tool (cvat)," 2018. [Online]. Available: <https://github.com/open-cv/cvat>
- [33] B. Wang, V. Wu, B. Wu, and K. Keutzer, "Latte: accelerating lidar point cloud annotation via sensor fusion, one-click annotation, and tracking," 2019. [Online]. Available: <https://arxiv.org/pdf/1904.09085>
- [34] W. Liu, D. Anguelov, D. Erhan, C. Szegedy, S. Reed, C.-Y. Fu, and A. C. Berg, "Ssd: single shot multibox detector," *European Conference on Computer Vision*, vol. 9905, pp. 21–37, 2016.
- [35] C. R. Qi, W. Liu, C. Wu, H. Su, and L. J. Guibas, "Frustum pointnets for 3d object detection from rgb-d data," 2017. [Online]. Available: <https://arxiv.org/pdf/1711.08488>
- [36] J. Uhrig, N. Schneider, L. Schneider, U. Franke, T. Brox, and A. Geiger, "Sparsity invariant cnns," 2017. [Online]. Available: <https://arxiv.org/pdf/1708.06500>
- [37] H. Caesar, V. Bankiti, A. H. Lang, S. Vora, V. E. Liong, Q. Xu, A. Krishnan, Y. Pan, G. Baldan, and O. Beijbom, "nusenes: A multimodal dataset for autonomous driving," 2019. [Online]. Available: <https://arxiv.org/abs/1903.11027>
- [38] H. A. Alhajja, S. K. Mustikovela, L. Mescheder, A. Geiger, and C. Rother, "Augmented reality meets computer vision: Efficient data generation for urban driving scenes," 2017. [Online]. Available: <https://arxiv.org/pdf/1708.01566>
- [39] J. Chang and G. Wetzstein, "Deep optics for monocular depth estimation and 3d object detection," 2019. [Online]. Available: <https://arxiv.org/pdf/1904.08601>